Published online 23 November 2017

Nucleic Acids Research, 2018, Vol. 46, No. 7 ***3543–3551***
doi: 10.1093/nar/gkx1185

DNA as UV light–harvesting antenna

Ivan L. Volkov[1], Zakhar V. Reveguk[1], Pavel Yu. Serdobintsev[1,2], Ruslan R. Ramazanov[1] and Alexei I. Kononov[1,*]

[1]St. Petersburg State University, St. Petersburg 199034, Russia and [2]St. Petersburg State Polytechnic University, St. Petersburg 195251, Russia

Received July 28, 2017; Revised November 08, 2017; Editorial Decision November 09, 2017; Accepted November 15, 2017

ABSTRACT

The ordered structure of UV chromophores in DNA resembles photosynthetic light-harvesting complexes in which quantum coherence effects play a major role in highly efficient directional energy transfer. The possible role of coherent excitons in energy transport in DNA remains debated. Meanwhile, energy transport properties are greatly important for understanding the mechanisms of photochemical reactions in cellular DNA and for DNA-based artificial nanostructures. Here, we studied energy transfer in DNA complexes formed with silver nanoclusters and with intercalating dye (acridine orange). Steady-state fluorescence measurements with two DNA templates (15-mer DNA duplex and calf thymus DNA) showed that excitation energy can be transferred to the clusters from 21 and 28 nucleobases, respectively. This differed from the DNA–acridine orange complex for which energy transfer took place from four neighboring bases only. Fluorescence up-conversion measurements showed that the energy transfer took place within ≲100 fs. The efficient energy transport in the Ag–DNA complexes suggests an excitonic mechanism for the transfer, such that the excitation is delocalized over at least four and seven stacked bases, respectively, in one strand of the duplexes stabilizing the clusters. This result demonstrates that the exciton delocalization length in some DNA structures may not be limited to just two bases.

INTRODUCTION

Coherent excitation transfer in photosynthesis is a clear example of quantum mechanical (QM) phenomena in living systems. In photosynthetic systems, nature has created an extremely intelligent light-harvesting system exhibiting unique quantum coherence properties and providing directional energy transport (1). Some simpler and more primitive photosystems, however, might have already appeared in the earliest stages of evolution. Under conditions of intense UV radiation, nucleic acids (NAs) might serve as UV light–harvesting molecules involved in some photochemical events in the prebiotic chemistry on Earth (2,3). A natural π-stacked system, a linear array of DNA bases has long been considered a possible pathway for charge (4–6) and excitation energy (7–9) transport. First, the charge and exciton transport properties are of great importance for understanding the mechanisms of photochemical reactions (10) in DNA, which lead to photodamage, carcinogenesis, and mutagenesis (11,12). DNA lesions caused by UV (13) and ionizing radiation (14) are in fact not random, and long-range energy transfer has been discussed as a possible explanation for the observed effects (8,14). Our recent theoretical study predicted that distorted base-stacking conformations exhibiting strongly red-shifted, low-energy excitonic states are especially susceptible to solar UV light-induced damage (15). These low-lying electronic states might act as traps for excitation energy. From a technological point of view, charge and excitation transfer in DNA are of clear interest in the developing area of DNA-based artificial nanostructures for nanophotonics and nanoelectronics applications (16). A lot of efforts have been made in the field of DNA-based light-harvesting antennas and wires using DNA as scaffold for functional molecules (17–24).

In NAs, the ordered structure of chromophores resembles the ordered pigments found in photosynthetic systems. As photosystem light-harvesting antennas, the absorption of a photon by NAs is of an excitonic nature, which clearly manifests in circular dichroism (CD) spectra (25). An exciton in the structure of ordered chromophores indicates a delocalization of the excitation. In this case, the energy transfer process can be quite different from non-coherent Förster and Dexter mechanisms (26). Kasha *et al.* described the basic principles of excitons in molecular aggregates (27), applying a theory of molecular Frenkel excitons in crystals developed by Davydov (28). Various theoretical approaches from the traditional Förster, Redfield and modified Redfield to generalized Förster (29–31) models have been developed to describe the excitation dynamics in molecular systems. Although wave-like behavior of the energy transport process in photosynthetic antennas has been proved experimentally (32,33), deriving an accurate theoretical descrip-

*To whom correspondence should be addressed. Tel: +7 8124289971; Fax: +7 8124287240; Email: a.kononov@spbu.ru

tion of excitation transfer dynamics remains a challenging task (1,34,35).

In NAs, exciton states might enhance energy transport in a similar manner to natural photosystems. Indeed, Markovitsi *et al.* observed energy transfer in DNA in time-resolved fluorescence anisotropy studies, even on femtosecond scale (36–38). The authors interpreted their results as evidence of exciton states in DNA. However, the length of the exciton delocalization remains uncertain. There have been no direct experimental observations of long-range delocalization of excitations in NAs so far, in contrast to photosynthetic light-harvesting systems, for which such observation have been made using nonlinear absorption and fast transient absorption pump–probe spectroscopy (39–41). Experimental evidence based on steady-state fluorescence excitation and CD spectra suggest that excitons in single-stranded NAs are limited to two bases (42–45). Based on UV/IR pump–probe experiments, Fiebig *et al.* suggested that an exciton is delocalized over 3–4 bases in polyadenines (46). However, Kohler *et al.* have refuted that result (47). Technical difficulties in the deep UV range and the heterogeneity of the studied systems hinder probing of the exciton dynamics in NAs. As an alternative approach, energy transfer experiments using bases as donors and NA-bound molecules as acceptors can be used to directly measure the distance and efficiency of the excitation energy migration and the exciton length in NAs. As the fluorescence lifetime of a major fraction of DNAs is typically hundreds of femtoseconds (36–38), efficient energy migration over large distances would clearly indicate the excitonic mechanism of the transfer and long-range exciton delocalization. However, experiments with intercalating dyes and with modified bases as energy acceptors have demonstrated energy transfer from the nearest neighboring bases only (8,48–51). This appears to support the view that the exciton is limited to a pair of bases. Obviously, long-range coherent effects do not play a major role in the relatively low-efficient energy trapping by the acceptors used in those systems. Meanwhile, theoretical calculations predict that excitons may extend over several DNA bases (52–56). All the acceptors used, however, nevertheless disrupt the native structure of DNA. Intercalators, for example, unwind DNA and the UV absorption band of modified bases usually overlaps poorly with the absorption spectra of the natural bases. Obviously, base–base and base–acceptor interactions are crucial for the energy transfer process in DNA–acceptor complexes. Can Frenkel exciton states in DNA be spread over more than two stacked bases?

In this study, we used a new class of acceptors, namely, metallic silver (Ag) nanoclusters, to study the process of energy transfer in DNA. Fluorescent Ag nanoclusters (57), and DNA-based Ag clusters (58–61) containing a few metallic atoms in particular, have attracted much attention in recent years because of their potential nanotechnology and nanomedicine applications. Gwinn and co-authors (62) showed that Ag clusters could act as acceptors of the electronic excitation in Ag–DNA complexes.

We synthesized Ag clusters stabilized by double-stranded regions of different DNA matrices, namely a 15-mer DNA duplex and natural calf thymus (CT) DNA. We demonstrate that excitation energy can be collected from 21 and 28 DNA nucleobases in the complexes formed by the Ag clusters with the 15-mer DNA and CT DNA, respectively. Femtosecond up-conversion measurements suggested that the energy transfer takes place within $\lesssim$100 fs. Our results indicate that the spatial extent of the exciton is four and seven bases, respectively, in the Ag–DNA complexes.

MATERIAL AND METHODS

Ag–DNA cluster synthesis

The PAGE purified oligonucleotide (5′-CGCCCCCCTCG GCGT-3′) was purchased from BioBeagle Ltd. (Saint-Petersburg, Russia); CT DNA was acquired from Sigma-Aldrich. In a typical preparation, DNA and $AgNO_3$ aqueous solutions were mixed and incubated for 15 min at room temperature. Next, $NaBH_4$ aqueous solution was added and stirred vigorously. For the oligonucleotide, the final concentrations were $C_{DNA} = 25\ \mu M$, $C_{AgNO3} = 150\ \mu M$ and $C_{NaBH4} = 75\ \mu M$. The solution was allowed to react in the dark for 2 h at room temperature. The purification of Ag clusters on the 15-mer DNA were performed as described in ref. (63). Ion-pair reversed-phase HPLC of the green-emitting Ag cluster was performed on a C18 column (Supelco Discovery, 250 × 4.6 mm, 5 μm; gradient B in A 1–50% in 30 min; A: 70 mM triethylammonium acetate aqueous buffer (pH 7.5); B: 70 mM triethylammonium acetate solution in methanol). The corresponding chromatograms are shown in Supplementary Figure S1. The purity of the isolated fraction was >90% as described in more detail in SI. Immediately after collection of the pure samples, they were solvent exchanged back to Milli-Q water by spin filtration with 3 kDa cut-off, which ensured that <1% of the HPLC running buffer remained.

CT DNA was subjected to 1-h thermal denaturation at 100°C, and snap-cooling in an ice-water bath. The CT DNA–water solution contained 5 mM $NaNO_3$ salt. For the CT DNA, the final concentrations were $C_{DNA} = 40\ \mu g/ml$, $C_{AgNO3} = 24\ \mu M$ and $C_{NaBH4} = 10\ \mu M$. The sample was kept in the dark for ∼1 week at 21°C to obtain a nearly homogeneous solution of 580 nm-emitting clusters. For fluorescence kinetics and saturation measurements Ag−DNA samples were concentrated using a vacuum centrifuge to enhance fluorescence signal.

Steady-state fluorescence measurements

Fluorescence spectra were obtained on a Fluorolog-3 (Horiba Jobin-Yvon) fluorometer in a 4-mm quartz cuvette at room temperature. The spectra were corrected for instrument sensitivity, polarization, and inner filter effects as described in SI. The quantum yield was measured by direct method using integrating sphere Quanta-φ.

Fluorescence up-conversion measurements

The fluorescence time-resolved measurements were made with a FOG 100-DX fluorescence up-conversion spectrometer (CDP System Corp., Moscow, Russia). The excitation was made by the third harmonic (266 nm) of a mode-locked Ti: sapphire laser (TISSA, CDP System Corp.) at 80 MHz. The 3-mm diameter 25-mW UV output beam was focused

by a 40-mm lens. Solutions were placed in a 2-mm rotating quartz cell. All measurements were performed at room temperature under aerated conditions. Photodegradation was <5% during a single scan. The apparatus function (IRF) was determined by measuring the Raman line signal in water. The IRF FWHM was typically ∼400 fs. The temporal resolution may be estimated as 100 fs in the sense that the components with less time cannot be resolved. A nonlinear fitting procedure was performed using single-exponential or double-exponential (when necessary) functions convoluted with the Gaussian apparatus function. The results are tabulated in Supplementary Table S1.

QM/MM simulations

The equilibrium structure of the Ag^+–DNA complex was obtained using QM/MM geometry optimization of the Ag ion–containing DNA duplex in explicit solvent using the CP2K program (64). In doing so, C–Ag^+–C pairs were taken in *trans* configuration because this conformation is energetically more favorable (65). The QM part of the system contained the nucleobases and Ag ions; the MM part contained the sugar–phosphate DNA backbone, a water shell (1 nm), and sodium (Na^+) ions as counterions. The model of the MM part used the parmbsc0 force field (66), periodic boundary conditions for orthogonal box 4 × 4 × 7 nm, and explicit TIP3P water solvent. Geometry relaxation of the QM part was performed using pseudopotential plane-wave density functional theory (DFT) in reciprocal space, namely pseudopotentials of Goedecker, Teter, and Hutter (GTH) (67) for core electrons, molecularly optimized DZVP-MOLOPT-GTH (68) basis set for valence electrons, and the GGA functional PBE (69) with D3 correction method of Grimme *et al.* (70). The full charges of the QM and MM parts were set to zero by removing redundant Na^+ ions. The same QM/MM simulations were performed with added Ag atoms at the C-T mismatches. A fragment comprising eight nucleobases and four Ag ions surrounded by the solvent shell was extracted from the equilibrium Ag^+–DNA structure. The number of Ag atoms and the charge of the cluster were varied until a reasonable agreement was achieved between the experimental and calculated excitation spectra. The excitation spectra of the cluster were calculated using the time-dependent (TD) DFT method. For the TDDFT calculations, meta-hybrid GGA functional M06–2x (71) and effective core potential def2-SVP (72) basis for Ag atoms used in the TURBOMOLE program (73) were used.

RESULTS

15-mer DNA duplex

The synthesis of DNA-stabilized Ag clusters typically results in a heterogeneous solution containing multiple species, most of them non-luminescent Ag–DNA complexes and bare DNA strands (60,74). In some cases, homogeneous solutions of fluorescent Ag–DNA complexes with defined cluster:DNA stoichiometry can be obtained via high-performance liquid chromatography (HPLC) purification (63). The absorption, fluorescence emission, and excitation spectra of the HPLC-purified complex of 15-mer DNA (5′-CGCCCCCCTCGGCGT-3′) and Ag clusters emitting at 560 nm are plotted in Figure 1. The quantum efficiency of the cluster at $\lambda_{ex} = 480$ nm is 10 ± 2%. The absorption extinction coefficient of the cluster at 485 nm was obtained directly using the fluorescence saturation method (SI, Supplementary Figure S5). It has been shown that two DNA strands stabilize the cluster (thus, cluster:DNA stoichiometry = 1:2) (63). The absorption spectrum of the bare DNA dimer with a known extinction coefficient (75) is also plotted in Figure 1. As seen in the figure, the UV band of the complex at 260 nm originates mainly from DNA absorption, while the band with a maximum at 485 nm is evidently from the lowest energy transition of the Ag cluster. The UV band observed in the excitation spectrum of the complex, as in other Ag–DNA complexes (62,74,76), is obviously due to energy transfer between DNA and the Ag cluster. Here, the excitation spectrum approaches its absorption spectrum, which indicates that the energy transfer efficiency is close to unity.

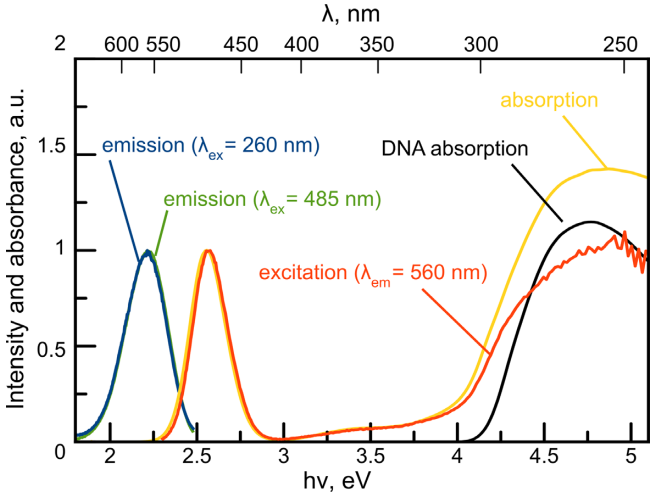

Figure 1. Fluorescence emission (blue and green), excitation (red), and absorption (yellow) spectra of HPLC-purified Ag–15-mer DNA (5′-CGCCCCCCTCGGCGT-3′) complex; the absorption spectrum of the DNA dimer template is in black. The excitation and absorption spectra of the Ag–DNA complex are normalized to 1 at visible maximum. The DNA absorption spectrum is plotted as the ratio of DNA extinction coefficient to the cluster extinction coefficient at visible maximum. The DNA extinction coefficient was calculated as described in ref. (75) (a hypochromic effect from G-C pairing in the dimer was also taken into account).

Quantitatively, the transfer efficiency φ can be estimated from the spectra shown in Figure 1, as follows (see SI):

$$\varphi = 1 - \frac{A(\lambda) - I(\lambda)}{A_{\mathrm{DNA}}(\lambda)}. \quad (1)$$

In this equation, the absorption $A(\lambda)$ and fluorescence excitation $I(\lambda)$ spectra of the Ag–DNA complex are normalized to 1 at visible maximum. The DNA absorption spectrum $A_{\mathrm{DNA}}(\lambda)$ is calculated as the ratio of DNA extinction coefficient ($\varepsilon_{\mathrm{DNA}}(\lambda)$) to the cluster extinction coefficient at visible maximum ($\varepsilon_{\mathrm{Ag}}^{\mathrm{max}}$). From the obtained spectral data, we derive the efficiency of the transfer $\varphi = 0.7 \pm 0.1$ for the excitation of the complex at 260 nm, which means that

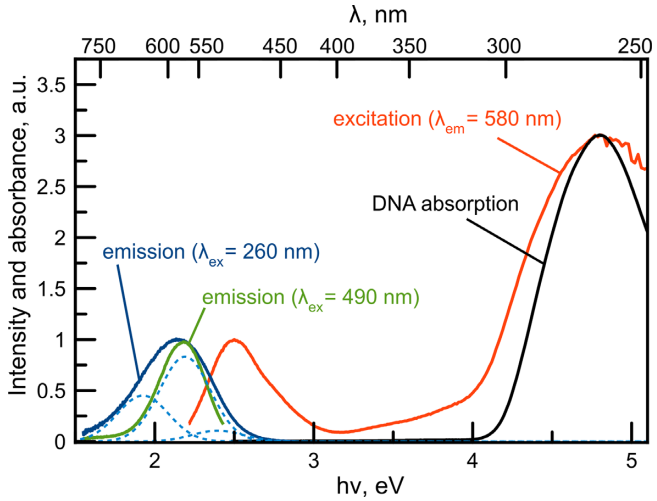

Figure 2. Fluorescence emission (blue and green), and excitation (red) spectra of Ag clusters bound to CT DNA; the absorption spectrum of the DNA template (scaled to the maximum of the UV excitation band) is in black. The emission spectrum of the complex excited at 260 nm (blue) was resolved into three Gaussians (dashed light blue).

21 ± 3 DNA bases (of 30 in the complex) transferred energy to the Ag cluster with 100% efficiency. Alternatively, it can be interpreted as the entire DNA duplex functioning as an antenna with 70% efficiency.

In our simple model, we neglected the base–cluster interaction that can affect the extinction coefficient of the DNA bases bound with Ag atoms. The total amount of the bases bound with the cluster is 8 of 30 in the duplex, as shown below. If, for example, the extinction coefficient for those bases differs by 50% from that in bare DNA, it will change the value of A_{DNA} by 13% and consequently φ by only 4%, which is within the experimental error of our measurements. A detailed investigation of the electronic states of the Ag–DNA complex would require robust QM calculations.

Calf thymus DNA

To estimate the possible length of the light-harvesting region in natural DNA, we synthesized fluorescent Ag clusters on CT DNA and applied a similar methodology to determine the number of bases transferring energy to the Ag clusters. It has been shown that complementary base-pairing hinders the formation of fluorescent Ag clusters (77). Therefore, CT DNA was first subjected to thermal denaturation, which also allowed us to obtain a more homogeneous solution of fluorescent species.

The fluorescence emission and excitation spectra of the Ag clusters on the CT DNA matrix are shown in Figure 2. The emission spectrum of the Ag–DNA complex exhibited an emission band at ca. 580 nm when excited at both 260 nm and 490 nm. The emission spectrum excited in the DNA band also exhibited the small presence of two other clusters in the blue and red regions that dominated at the earlier and later stages of synthesis, respectively (the spectrum excited at 260 nm is resolved into three bands, as shown in Figure 2).

The fluorescence excitation band with maximum at 260 nm nearly coincides with the DNA absorption spectrum, which suggests that energy transfer from the DNA bases excited the fluorescence of the Ag clusters. As with the Ag cluster on 15-mer DNA, the intrinsic absorption of the cluster at 260 nm is probably not significant with respect to the absorption of DNA bases sensitizing the emission of the Ag cluster. If so, then the number of DNA bases transferring energy N can be estimated from the UV and visible band intensity ratio in the fluorescence excitation spectrum of the cluster using the following equation (see SI):

$$N = \frac{I(260) \cdot f \cdot \varepsilon_{Ag}^{max}}{\varepsilon_{DNA\ b.}(260) \cdot \varphi}, \quad (2)$$

where $I(260)$ denotes the intensity at 260 nm in the excitation spectrum normalized to 1 at visible peak, f the fractional intensity of the cluster at the emission maximum at 580 nm, $\varepsilon_{DNA\ b.}(260)$ the extinction coefficient of DNA bases at 260 nm, and φ the transfer efficiency.

We obtained the value $\varepsilon_{Ag}^{max} = (1.0 \pm 0.1) \times 10^5$ $M^{-1}cm^{-1}$ at 490 nm using fluorescence saturation spectroscopy (76) (see SI, Supplementary Figure S6). Taking a typical value of $\varepsilon_{DNA\ b.}(260) = 6.6 \times 10^3$ $M^{-1}cm^{-1}$ for CT DNA, $f = 0.8$ obtained from the three-Gaussian approximation (Figure 2), and assuming 100% efficiency for the transfer, we obtained $N = 35 \pm 3$ bases. This value is probably slightly overestimated due to the contribution of the intrinsic absorption of the Ag cluster to the excitation spectrum of the complex. If this contribution, as with the 15-mer DNA, is ~20%, it reduces N to 28 bases. It is also worth noting that if the transfer efficiency is <100%, the value of N will be greater.

Energy transfer between DNA bases and intercalated dyes

Further, we compared energy transfer efficiencies in the DNA complexes with Ag clusters and intercalating dyes as acceptors. We estimated the energy transfer range in the CT DNA–acridine orange (AO) complex with the same method as for Ag clusters. As before, we paid special attention to possible artefacts affecting the value of N, such as polarization effects, scattering light, and instrument correction, as described in SI. Figure 3 shows the fluorescence emission and excitation spectra of the AO–DNA complex and the absorption spectrum of AO in the complex obtained as the differential AO–DNA/DNA spectrum. At the AO/DNA ratio used (0.01), AO is bound with DNA by intercalation (78). The AO–DNA complex exhibits a typical spectral shift of both excitation and emission maxima in comparison with AO solution (Supplementary Figure S7). To estimate the number of bases transferring the energy to the dye, we used the same Equation (2), where $I(260)$ now denotes the difference between the excitation spectrum of the AO–DNA complex and the AO absorption spectrum normalized to 1 at visible peak, $f = 1$, and ε_{Ag}^{max} is replaced by the extinction coefficient for AO at the visible maximum (6×10^4 M^{-1} cm^{-1} (79,80)); we obtained $N = 4.3 \pm 0.5$ bases. This value means that energy transfer in the AO–DNA complex proceeded from the four nearest neighboring bases (being in van der Waals contact with the dye) in the double-stranded

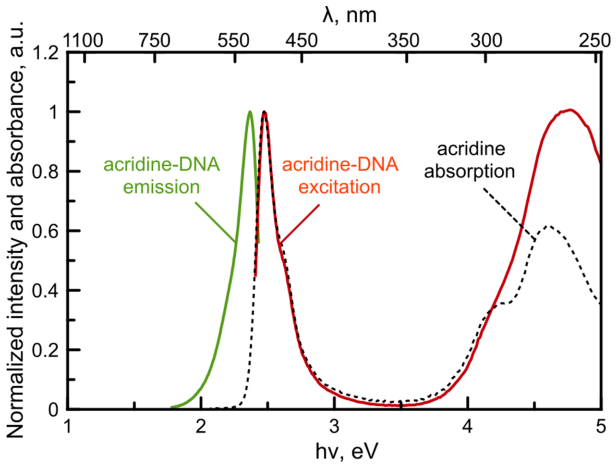

Figure 3. Fluorescence emission (green) and excitation (red) spectra of AO–DNA complex; dashed line indicates differential AO–DNA/DNA spectrum.

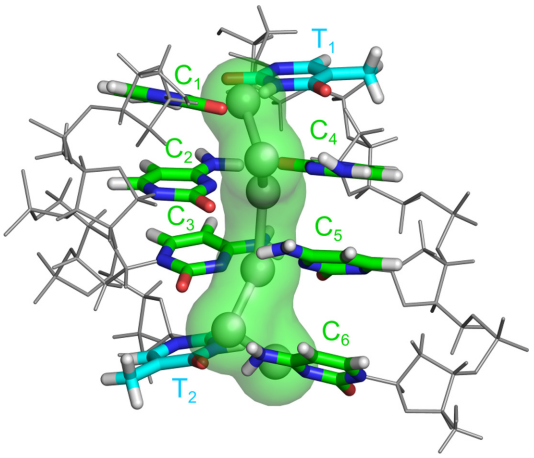

Figure 4. QM/MM optimized structure of the chromophoric core of the complex of Ag_6^{2+} cluster with 15-mer DNA duplex.

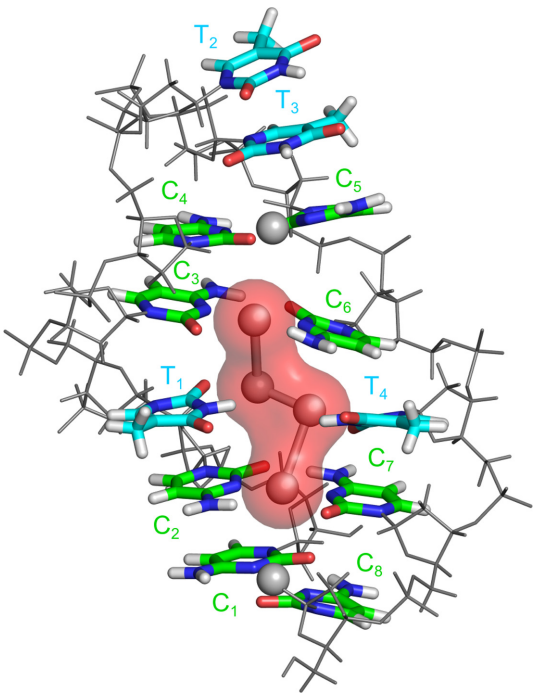

Figure 5. Structure of Ag_4^{2+} cluster stabilized by double-stranded region of DNA hairpin (74).

DNA, which is in agreement with other studies on energy transfer in similar DNA–acceptor systems (48–51).

Structure of Ag–DNA complexes

To determine the possible energy transfer distances and to examine whether the size of the Ag clusters is indeed smaller than the DNA region responsible for light-harvesting in the Ag–DNA complexes, we modeled the structure of the complexes. The structure of the cluster on the 15-mer DNA was obtained using the same algorithm proposed in (74) for an Ag_4^{+2} cluster. In the first stage, we obtained the QM/MM-optimized structure of the Ag^+-DNA precursor. In doing so, we considered the earlier established fact that the emitting Ag–15-mer DNA complex is a strand dimer complex (63). The optimized equilibrium structure of the 15-mer DNA duplex stabilized by Ag^+ cations was obtained by QM/MM simulation (Supplementary Figure S8). This structure resembles a recently reported crystal structure of a Ag^+–DNA nanowire (81). Then, DNA sequence modifications allowed us to determine the probable binding sites of the cluster. It appears that replacing thymine with cytosine in the middle of the sequence led to the disappearance of the 560 nm emission (Supplementary Figure S9). This suggests that Ag atoms are located at the C-T mismatches, as was the case for the Ag_4^{2+} cluster on the 12-mer DNA (74) and Ag clusters on the DNA duplex (77). Subsequently, QM/MM simulations of the system were performed with added Ag atoms at the C–T mismatches. We added Ag atoms in such a way that initial cluster structures had elongated shapes. The number of Ag atoms and the charge were varied in the ranges of 4–8 and 0 to +3 respectively based on our previous calculations of threadlike Ag clusters (82,83). It appeared that only Ag_6^{2+} cluster had excitation spectrum close to the experimental one. The optimized structure obtained for the chromophoric core of the green-emitting Ag_6^{2+}–DNA complex is presented in Figure 4. The calculated excitation spectrum of the Ag_6^{2+} cluster is shown in Supplementary Figure S10. The predicted larger size of this cluster compared to the Ag_4^{2+} cluster correlates well with the fact that it has two times higher experimental absorption cross-section (2.0×10^5 M^{-1} cm^{-1}) than the Ag_4^{2+} cluster (1.0×10^5 M^{-1} cm^{-1} (76)).

The cluster on the CT DNA exhibited the same absorption cross-section and similar spectral properties as the reported earlier Ag_4^{2+} cluster on the 12-mer DNA (74,76). As the spectral parameters of Ag clusters are extremely sensitive to size, charge, and shape (83–85), we believe that these Ag–DNA complexes have a similar metal acceptor core structures.

Figure 5 shows that the Ag_4^{2+} cluster is also stabilized by two DNA strands at a mismatch site. Of course, the base sequence may differ in the case of the CT DNA.

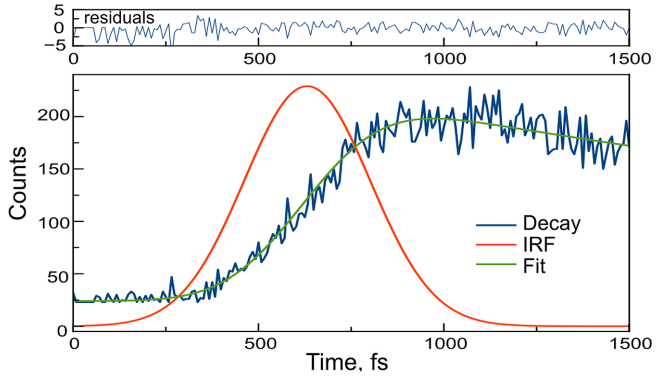

Figure 6. Fluorescence rise curve at 590 nm of Ag clusters bound to CT DNA (λ_{ex} = 266 nm); fit: exp(-t/3 ps). No rise component is resolved within the time resolution of the instrument (~100 fs).

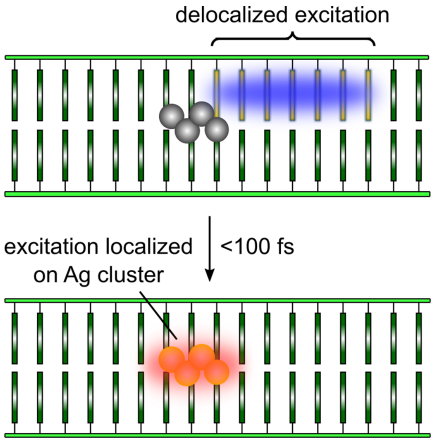

Figure 7. The excitation transfer process between DNA bases and the emitting DNA duplex–bound Ag cluster. Vertical bars represent DNA bases in the duplex, gray circles represent the cluster bound with six bases, the blue oval area shows the spatial extent of the exciton, and the red oval area illustrates localization of the excitation on the cluster.

Rate of energy transfer

To clarify the mechanism of energy transfer in the DNA–metal acceptor complexes, we determined the energy transfer rate by performing a series of fluorescence kinetics measurements. First, we measured the fluorescence lifetime of the bare CT DNA and 15-mer oligonucleotide used for synthesizing the fluorescent Ag–DNA complexes. The fluorescence decay trace of the 15-mer DNA at 325 nm in a 5-ps time window is shown in Supplementary Figure S11. An appropriate two-exponential fit yielded a major decay component of 380 fs. The excited state of the major fraction of CT DNA decayed with a lifetime of 490 fs (Supplementary Figure S12). The high energy transfer efficiency between donor and acceptor implies a relatively high rate of transfer with respect to the donor excited state lifetime. In general, the energy transfer efficiency is determined as follows (86):

$$\varphi = \frac{k_{ET}}{k_{ET} + k}, \quad (3)$$

where k_{ET} is the rate of energy transfer and k is the intrinsic rate of donor deactivation. At the given rate of DNA deactivation of (380 fs)$^{-1}$ and $\varphi = 0.7$ for the 15-mer DNA, it follows that the transfer should proceed within <160 fs.

The rate of the energy transfer from DNA to the cluster could be directly measured as the rise time of the cluster fluorescence when DNA was excited. Figure 6 shows the fluorescence rise trace of the cluster on the CT DNA with excitation at 266 nm (within the DNA absorption band). At the available time resolution of the instrument of ca. 100 fs, one can state that the energy transfer indeed occurs at <100 fs.

DISCUSSION

The number of nucleobases collecting the excitation energy in the complexes of Ag clusters with CT DNA and 15-mer DNA duplex appears to be 5–7 times greater than the typical values observed for DNA–acceptor systems (8,48–51) and three-fold greater than that estimated earlier for a 23-mer (62) hairpin with about 10 bases in the stem. As Ag clusters bind to 6–8 DNA bases in the double-stranded regions (Figures 4 and 5), it would be reasonable to expect an energy transfer from 6–8 DNA bases. With relatively long double-stranded regions (as in CT DNA or the 15-mer duplex), however, energy transfer involves 21–28 bases as the donors, most of them distal from the cluster. Hence, the energy transport through the DNA stack contributes significantly to the energy transfer process. The fast rate of the transfer of $\gtrsim$(100 fs)$^{-1}$ at a distance of about 25 Å (half the length of the 15-mer duplex) is evidently incompatible with a trivial, non-coherent Förster mechanism. Such ultrafast (and thus highly efficient) energy transfer requires delocalization of the excitation between DNA bases not bound with Ag atoms and at least one base bound with an Ag cluster. It is most likely that excitation is delocalized over DNA bases in one strand. Then, to collect the excitation energy from DNA bases not bound with Ag clusters, the minimum necessary exciton size (M) in each of four single-strand DNA segments adjacent to the cluster can be estimated as:

$$M = \frac{N - n}{4} + 1, \quad (4)$$

where N denotes the number of bases transferring energy and n the number of bases bound with Ag clusters. In the case of the 15-mer DNA duplex, $N = 21$ and $n = 8$. M thus estimated appears to be four bases. For the CT DNA, $N = 28$ and $n = 6$, and M is about seven bases. The latter scenario is schematically illustrated in Figure 7.

Both cases differ significantly from the complex with AO, which did not indicate any delocalization. Of course, local DNA structure as well as base composition may differ in those cases. Experimentally, delocalization of the excitation might manifest in the transient absorption spectra in a time domain shorter than the time of exciton localization. Enhancement of the ground-state bleaching due to exciton delocalization was observed in photosynthetic light-harvesting systems (39,40) and in dye–DNA complexes (87). Meanwhile, no enhancement has been observed in the transient absorption spectra reported in the literature for polymeric NA components compared to monomers, and at

least at the time of ∼100 fs (instrument time resolution) after the pulse, the ground-state absorption bleaching is the same as that of the monomers (47,88). This might indicate that exciton localization occurs faster than 100 fs. In this respect, pump–probe experiments with 10-fs time resolution in the deep UV range remain challenging.

CONCLUSION

We observed ultrafast, efficient energy transfer in the complexes of Ag clusters with a 15-mer DNA duplex and CT DNA. The excitation energy was transferred from 21 and 28 DNA bases, respectively, to the fluorescent clusters in the double-stranded regions. Such efficient energy transport can be explained by delocalization of the excitation over four and seven stacked bases in one of the four single-strand DNA segments, followed by energy transfer to the lowest excited state of the cluster within ≲100 fs. This result demonstrates that the exciton delocalization length in some DNA structures may not be limited to just two bases. Direct evidence for the quantum wave–like nature of the energy transfer might be obtained in a time domain shorter than 100 fs, which remains challenging in the deep UV range. The result obtained in the present study prompts further efforts in probing the ultrafast dynamics of excitation in NAs. We are at the very threshold of understanding of the role of quantum effects in biology, and Frenkel excitons in DNA may yet be one more possible instance of coherent processes in biosystems.

SUPPLEMENTARY DATA

Supplementary Data are available at NAR online.

ACKNOWLEDGEMENTS

This work was carried out using equipment of Centre for Optical and Laser Materials Research and of Chemical Analysis and Materials Research Centre of St. Petersburg State University. We also thank CDP Systems Corp. for assistance in femtosecond measurements. The reported calculations were performed in the Supercomputing Center of Lomonosov Moscow State University.

FUNDING

Russian Science Foundation (RSF) [16-13-10090]. Funding for open access charge: RSF [16-13-10090].
Conflict of interest statement. None declared.

REFERENCES

1. Fassioli,F., Dinshaw,R., Arpin,P.C. and Scholes,G.D. (2014) Photosynthetic light harvesting: excitons and coherence. *J. R. Soc. Interface*, **11**, 20130901.
2. Sagan,C. (1973) Ultraviolet selection pressure on the earliest organisms. *J. Theor. Biol.*, **39**, 195–200.
3. Skulachev,V.P. (1994) Bioenergetics: the evolution of molecular mechanisms and the development of bioenergetic concepts. *Antonie Van Leeuwenhoek*, **65**, 271–284.
4. Livshits,G.I., Stern,A., Rotem,D., Borovok,N., Eidelshtein,G., Migliore,A., Penzo,E., Wind,S.J., Di Felice,R., Skourtis,S.S. *et al.* (2014) Long-range charge transport in single G-quadruplex DNA molecules. *Nat. Nanotechnol.*, **9**, 1040–1046.
5. Slinker,J.D., Muren,N.B., Renfrew,S.E. and Barton,J.K. (2011) DNA charge transport over 34 nm. *Nat. Chem.*, **3**, 228–233.
6. Schuster,G.B. (ed). (2004) *Longe-Range Charge Transfer in DNA I Springer Berlin Heidelberg*, Berlin, Heidelberg.
7. Guéron,M., Eisinger,J. and Lamola,A.A. (1974) 4-Excited states of nucleic acids. In: *Basic Principles in Nucleic Acid Chemistry*. pp. 311–398.
8. Nordlund,T.M. (2007) Sequence, structure and energy transfer in DNA. *Photochem. Photobiol.*, **83**, 625–636.
9. Middleton,C.T., de La Harpe,K., Su,C., Law,Y.K., Crespo-Hernández,C.E. and Kohler,B. (2009) DNA excited-state dynamics: from single bases to the double helix. *Annu. Rev. Phys. Chem.*, **60**, 217–239.
10. Cadet,J., Mouret,S., Ravanat,J.L. and Douki,T. (2012) Photoinduced damage to cellular DNA: Direct and photosensitized reactions. *Photochem. Photobiol.*, **88**, 1048–1065.
11. Pfeifer,G.P., You,Y.-H. and Besaratinia,A. (2005) Mutations induced by ultraviolet light. *Mutat. Res.*, **571**, 19–31.
12. De Gruijl,F.R. (1999) Skin cancer and solar UV radiation. *Eur. J. Cancer*, **35**, 2003–2009.
13. Brash,D.E. and Haseltine,W.A. (1982) UV-induced mutation hotspots occur at DNA damage hotspots. *Nature*, **298**, 189–192.
14. Baverstock,K.F. and Cundall,R.B. (1988) Solitons and energy transfer in DNA. *Nature*, **332**, 312–313.
15. Ramazanov,R.R., Maksimov,D.A. and Kononov,A.I. (2015) Noncanonical stacking geometries of nucleobases as a preferred target for solar radiation. *J. Am. Chem. Soc.*, **137**, 11656–11665.
16. Stulz,E. (2012) DNA Architectonics: towards the Next Generation of Bio-inspired Materials. *Chem. - A Eur. J.*, **18**, 4456–4469.
17. Varghese,R. and Wagenknecht,H.-A. (2009) DNA as a supramolecular framework for the helical arrangements of chromophores: towards photoactive DNA-based nanomaterials. *Chem. Commun.*, **19**, 2615–2624.
18. Dutta,P.K., Varghese,R., Nangreave,J., Lin,S., Yan,H. and Liu,Y. (2011) DNA-directed artificial light-harvesting antenna. *J. Am. Chem. Soc.*, **133**, 11985–11993.
19. Garo,F. and Häner,R. (2012) A DNA-based light-harvesting antenna. *Angew. Chemie - Int. Ed.*, **51**, 916–919.
20. Teo,Y.N. and Kool,E.T. (2012) DNA-multichromophore systems. *Chem. Rev.*, **112**, 4221–4245.
21. Asanuma,H., Fujii,T., Kato,T. and Kashida,H. (2012) Coherent interactions of dyes assembled on DNA. *J. Photochem. Photobiol. C Photochem. Rev.*, **13**, 124–135.
22. Albinsson,B., Hannestad,J.K. and Börjesson,K. (2012) Functionalized DNA nanostructures for light harvesting and charge separation. *Coord. Chem. Rev.*, **256**, 2399–2413.
23. Toppari,J.J., Wirth,J., Garwe,F., Stranik,O., Csaki,A., Bergmann,J., Paa,W. and Fritzsche,W. (2013) Plasmonic coupling and long-range transfer of an excitation along a DNA nanowire. *ACS Nano*, **7**, 1291–1298.
24. Pan,K., Boulais,E., Yang,L. and Bathe,M. (2014) Structure-based model for light-harvesting properties of nucleic acid nanostructures. *Nucleic. Acids. Res.*, **42**, 2159–2170.
25. Bush,C.A. (1974) Uv spectroscopy circular dichroism and optical rotatory dispersion. *Ts'o, Paul O P Basic Princ. Nucleic Acid Chem.* Acad. Press. Inc., Vol. **2**.
26. Scholes,G.D., Fleming,G.R., Olaya-Castro,A. and van Grondelle,R. (2011) Lessons from nature about solar light harvesting. *Nat. Chem.*, **3**, 763–774.
27. Kasha,M., Rawls,H.R. and Ashraf El-Bayoumi,M. (1965) The exciton model in molecular spectroscopy. *Pure Appl. Chem.*, **11**, 371–392.
28. Davydov,A. (1962) *Theory of Molecular Excitons*. McGraw-Hill, NY.
29. May,V., Kühn,O. and Wiley InterScience (Online service) (2000) *Charge and Energy Transfer Dynamics in Molecular Systems Wiley-VCH*, Berlin.
30. Yang,M. and Fleming,G.R. (2002) Influence of phonons on exciton transfer dynamics: comparison of the Redfield, Förster, and modified Redfield equations. *Chem. Phys.*, **275**, 355–372.
31. Strümpfer,J. and Schulten,K. (2009) Light harvesting complex II B850 excitation dynamics. *J. Chem. Phys.*, **131**, 225101.
32. Collini,E., Wong,C.Y., Wilk,K.E., Curmi,P.M.G., Brumer,P. and Scholes,G.D. (2010) Coherently wired light-harvesting in

photosynthetic marine algae at ambient temperature. *Nature*, **463**, 644–647.
33. Engel,G.S., Calhoun,T.R., Read,E.L., Ahn,T.-K., Mancal,T., Cheng,Y.-C., Blankenship,R.E. and Fleming,G.R. (2007) Evidence for wavelike energy transfer through quantum coherence in photosynthetic systems. *Nature*, **446**, 782–786.
34. Novoderezhkin,V.I. and van Grondelle,R. (2010) Physical origins and models of energy transfer in photosynthetic light-harvesting. *Phys. Chem. Chem. Phys.*, **12**, 7352–7365.
35. Strümpfer,J., Şener,M. and Schulten,K. (2012) How quantum coherence assists photosynthetic light-harvesting. *J. Phys. Chem. Lett.*, **3**, 536–542.
36. Gustavsson,T., Banyasz,A., Improta,R. and Markovitsi,D. (2011) Femtosecond fluorescence studies of DNA/RNA constituents. *J. Phys. Conf. Ser.*, **261**, 12009.
37. Vayá,I., Gustavsson,T., Douki,T., Berlin,Y. and Markovitsi,D. (2012) Electronic excitation energy transfer between nucleobases of natural DNA. *J. Am. Chem. Soc.*, **134**, 11366–11368.
38. Markovitsi,D. (2016) UV-induced DNA damage: the role of electronic excited states. *Photochem. Photobiol.*, **92**, 45–51.
39. Novoderezhkin,V.I. and Razjivin,A.P. (1993) Excitonic interactions in the light-harvesting antenna of photosynthetic purple bacteria and their influence on picosecond absorbency difference spectra. *FEBS Lett.*, **330**, 5–7.
40. Novoderezhkin,V., Monshouwer,R. and van Grondelle,R. (1999) Exciton (de)localization in the LH2 antenna of Rhodobacter sphaeroides as revealed by relative difference absorption measurements of the LH2 antenna and the B820 subunit. *J. Phys. Chem. B*, **103**, 10540–10548.
41. Leupold,D., Stiel,H., Teuchner,K., Nowak,F., Sandner,W., Ücker,B. and Scheer,H. (1996) Size enhancement of transition dipoles to one- and two-exciton bands in a photosynthetic antenna. *Phys. Rev. Lett.*, **77**, 4675–4678.
42. Kononov,A.I., Bakulev,V.M. and Rapoport,V.L. (1993) Exciton effects in dinucleotides and polynucleotides. *J. Photochem. Photobiol. B Biol.*, **19**, 139–144.
43. Kadhane,U., Holm,A.I.S., Hoffmann,S.V. and Nielsen,S.B. (2008) Strong coupling between adenine nucleobases in DNA single strands revealed by circular dichroism using synchrotron radiation. *Phys. Rev. E*, **77**, 21901–21904.
44. Holm,A.I.S., Nielsen,L.M., Kohler,B., Hoffmann,S.V. and Nielsen,S.B. (2010) Electronic coupling between cytosine bases in DNA single strands and i-motifs revealed from synchrotron radiation circular dichroism experiments. *Phys. Chem. Chem. Phys.*, **12**, 3426–3430.
45. Nielsen,L.M., Hoffmann,S.V. and Nielsen,S.B. (2013) Electronic coupling between photo-excited stacked bases in DNA and RNA strands with emphasis on the bright states initially populated. *Photochem. Photobiol. Sci.*, **12**, 1273–1285.
46. Buchvarov,I., Wang,Q., Raytchev,M., Trifonov,A. and Fiebig,T. (2007) Electronic energy delocalization and dissipation in single- and double-stranded DNA. *Proc. Natl. Acad. Sci. U.S.A.*, **104**, 4794–4797.
47. Su,C., Middleton,C.T. and Kohler,B. (2012) Base-stacking disorder and excited-state dynamics in single-stranded adenine homo-oligonucleotides. *J. Phys. Chem. B*, **116**, 10266–10274.
48. Rayner,D.M., Szabo,A.G., Loutfy,R.O. and Yip,R.W. (1980) Singlet energy transfer between nucleic acid bases and dyes in intercalation complexes. *J. Phys. Chem.*, **84**, 289–293.
49. Georghiou,S., Zhu,S., Weidner,R., Huang,C.R. and Ge,G. (1990) Singlet-singlet energy transfer along the helix of a double-stranded nucleic acid at room temperature. *J. Biomol. Struct. Dyn.*, **8**, 657–674.
50. Rist,M., Wagenknecht,H.-A. and Fiebig,T. (2002) Exciton and excimer formation in DNA at room temperature. *ChemPhysChem*, **3**, 704–707.
51. Dumas,A. and Luedtke,N.W. (2011) Highly fluorescent guanosine mimics for folding and energy transfer studies. *Nucleic Acids Res.*, **39**, 6825–6834.
52. Bouvier,B. and Dognon,J.P. (2003) Influence of conformational dynamics on the exciton states of DNA oligomers. *J. Phys. Chem. B*, **107**, 13512–13522.
53. Vayá,I., Brazard,J., Huix-Rotllant,M., Thazhathveetil,A.K., Lewis,F.D., Gustavsson,T., Burghardt,I., Improta,R. and Markovitsi,D. (2016) High-energy long-lived mixed Frenkel-charge-transfer excitons: From double stranded (AT)n to natural DNA. *Chem. - A Eur. J.*, **22**, 4904–4914.
54. Huix-Rotllant,M., Brazard,J., Improta,R., Burghardt,I. and Markovitsi,D. (2015) Stabilization of mixed Frenkel-charge transfer excitons extended across both strands of guanine–cytosine DNA duplexes. *J. Phys. Chem. Lett.*, **6**, 2247–2251.
55. Emanuele,E., Zakrzewska,K., Markovitsi,D., Lavery,R. and Millie,P. (2005) Exciton states of dynamic DNA double helices: alternating dCdG sequences. *J. Phys. Chem. B*, **109**, 16109–16118.
56. Czader,A. and Bittner,E.R. (2008) Calculations of the exciton coupling elements between the DNA bases using the transition density cube method. *J. Chem. Phys.*, **128**, 35101.
57. Choi,S., Dickson,R.M. and Yu,J. (2012) Developing luminescent silver nanodots for biological applications. *Chem. Soc. Rev.*, **41**, 1867–1891.
58. Petty,J.T., Story,S.P., Hsiang,J.C. and Dickson,R.M. (2013) DNA-templated molecular silver fluorophores. *J. Phys. Chem. Lett.*, **4**, 1148–1155.
59. Obliosca,J.M., Liu,C., Batson,R.A., Babin,M.C., Werner,J.H. and Yeh,H.C. (2013) DNA/RNA detection using DNA-templated few-atom silver nanoclusters. *Biosensors*, **3**, 185–200.
60. Gwinn,E., Schultz,D., Copp,S. and Swasey,S. (2015) DNA-protected silver clusters for nanophotonics. *Nanomaterials*, **5**, 180–207.
61. Thyrhaug,E., Bogh,S.A., Carro-Temboury,M.R., Madsen,C.S., Vosch,T. and Zigmantas,D. (2017) Ultrafast coherence transfer in DNA-templated silver nanoclusters. *Nat. Commun.*, **8**, 1–7.
62. O'Neill,P.R., Gwinn,E.G., Fygenson,D.K. and O'Neill,P.R. (2011) UV excitation of DNA stabilized Ag cluster fluorescence via the DNA bases. *J. Phys. Chem. C*, **115**, 24061–24066.
63. Schultz,D. and Gwinn,E.G. (2012) Silver atom and strand numbers in fluorescent and dark Ag:DNAs. *Chem. Commun. (Cambridge, England).*, **48**, 5748–5750.
64. VandeVondele,J., Krack,M., Mohamed,F., Parrinello,M., Chassaing,T. and Hutter,J. (2005) Quickstep: fast and accurate density functional calculations using a mixed Gaussian and plane waves approach. *Comput. Phys. Commun.*, **167**, 103–128.
65. Megger,D.A. and Muller,J. (2010) Silver(I)-mediated cytosine self-pairing is preferred over hoogsteen-type base pairs with the artificial nucleobase 1,3-dideaza-6-nitropurine. *Nucleosides Nucleotides Nucleic Acids*, **29**, 27–38.
66. Pérez,A., Marchán,I., Svozil,D., Sponer,J., Cheatham,T.E., Laughton,C.A., Orozco,M., Pe,A. and Cheatham,T.E. III (2007) Refinement of the AMBER force field for nucleic acids: improving the description of alpha/gamma conformers. *Biophys. J.*, **92**, 3817–3829.
67. Goedecker,S., Teter,M. and Hutter,J. (1996) Separable dual-space Gaussian pseudopotentials. *Phys. Rev. B*, **54**, 1703–1710.
68. VandeVondele,J. and Hutter,J. (2007) Gaussian basis sets for accurate calculations on molecular systems in gas and condensed phases. *J. Chem. Phys.*, **127**, 114105–114109.
69. Perdew,J.P., Burke,K. and Ernzerhof,M. (1996) Generalized gradient approximation made simple. *Phys. Rev. Lett.*, **77**, 3865–3868.
70. Grimme,S., Antony,J., Ehrlich,S. and Krieg,H. (2010) A consistent and accurate ab initio parametrization of density functional dispersion correction (DFT-D) for the 94 elements H-Pu. *J. Chem. Phys.*, **132**, 154104.
71. Zhao,Y. and Truhlar,D.G. (2008) The M06 suite of density functionals for main group thermochemistry, thermochemical kinetics, noncovalent interactions, excited states, and transition elements: two new functionals and systematic testing of four M06-class functionals and 12 other function. *Theor. Chem. Acc.*, **120**, 215–241.
72. Weigend,F. and Ahlrichs,R. (2005) Balanced basis sets of split valence, triple zeta valence and quadruple zeta valence quality for H to Rn: design and assessment of accuracy. *Phys. Chem. Chem. Phys.*, **7**, 3297–3305.
73. Furche,F., Ahlrichs,R., Hättig,C., Klopper,W., Sierka,M. and Weigend,F. (2014) Turbomole. *Wiley Interdiscip. Rev. Comput. Mol. Sci.*, **4**, 91–100.
74. Ramazanov,R.R., Sych,T.S., Reveguk,Z.V., Maksimov,D.A., Vdovichev,A.A. and Kononov,A.I. (2016) Ag–DNA emitter: metal nanorod or supramolecular complex? *J. Phys. Chem. Lett.*, **7**, 3560–3566.

75. Tataurov,A.V., You,Y. and Owczarzy,R. (2008) Predicting ultraviolet spectrum of single stranded and double stranded deoxyribonucleic acids. *Biophys. Chem.*, **133**, 66–70.
76. Volkov,I., Sych,T., Serdobintsev,P., Reveguk,Z. and Kononov,A. (2016) Fluorescence saturation spectroscopy in probing electronically excited states of silver nanoclusters. *J. Lumin.*, **172**, 175–179.
77. Huang,Z., Pu,F., Hu,D., Wang,C., Ren,J. and Qu,X. (2011) Site-specific DNA-programmed growth of fluorescent and functional silver nanoclusters. *Chemistry*, **17**, 3774–3780.
78. Fredericq,E. and Houssier,C. (1972) Study of the interaction of DNA and acridine orange by various optical methods. *Biopolymers*, **11**, 2281–2308.
79. Armstrong,R.W., Kurucsev,T. and Strauss,U.P. (1970) The interaction between acridine dyes and deoxyribonucleic acid. *J. Am. Chem. Soc.*, **92**, 3174–3181.
80. Robinson,B.H., Löffler,A. and Schwarz,G. (1973) Thermodynamic behaviour of acridine orange in solution. Model system for studying stacking and charge-effects on self-aggregation. *J. Chem. Soc. Faraday Trans. 1 Phys. Chem. Condens. Phases*, **69**, 56–69.
81. Kondo,J., Tada,Y., Dairaku,T., Hattori,Y., Saneyoshi,H., Ono,A. and Tanaka,Y. (2017) A metallo-DNA nanowire with uninterrupted one-dimensional silver array. *Nat. Chem.*,**9**, 956–960.
82. Maksimov,D.A., Pomogaev,V.A. and Kononov,A.I. (2017) Excitation spectra of Ag3–DNA bases complexes: a benchmark study. *Chem. Phys. Lett.*, **673**, 11–18.
83. Ramazanov,R.R. and Kononov,A.I. (2013) Excitation spectra argue for threadlike shape of DNA-stabilized silver fluorescent clusters. *J. Phys. Chem. C*, **117**, 18681–18687.
84. Guidez,E.B. and Aikens,C.M. (2012) Theoretical analysis of the optical excitation spectra of silver and gold nanowires. *Nanoscale*, **4**, 4190–4198.
85. Swasey,S.M., Karimova,N., Aikens,C.M., Schultz,D.E., Simon,A.J. and Gwinn,E.G. (2014) Chiral electronic transitions in fluorescent silver clusters stabilized by DNA. *ACS Nano*, **8**, 6883–6892.
86. Valeur,B. and Berberan-Santos,M.N. (2012) *Molecular Fluorescence: Principles and Applications*, 2nd edn. Wiley-VCH Verlag GmbH & Co. KGaA, Weinheim.
87. Kononov,A.I., Moroshkina,E.B., Tkachenko,N.V. and Lemmetyinen,H. (2001) Photophysical processes in the complexes of DNA with ethidium bromide and acridine orange: a femtosecond study. *J. Phys. Chem. B*, **105**, 535–541.
88. Crespo-Hernández,C.E., Cohen,B. and Kohler,B. (2005) Base stacking controls excited-state dynamics in A.T DNA. *Nature*, **436**, 1141–1144.